



Cite this: *Chem. Commun.*, 2025, 61, 7486

Received 26th March 2025,  
Accepted 22nd April 2025

DOI: 10.1039/d5cc01702e

rsc.li/chemcomm

# Photocatalytic oxidation of biologically relevant reducing agents by $[\text{Ru}(\text{bpy})_3](\text{PF}_6)_2$ <sup>†</sup>

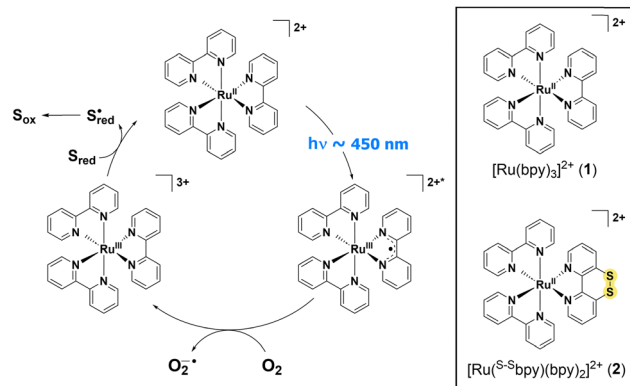
Iman Doumi,<sup>ib</sup> ‡<sup>a</sup> Daniella Al Othman,<sup>‡a</sup> Shao-An Hua,<sup>bc</sup> Vincent Lebrun,<sup>ib</sup> <sup>a</sup>  
Franc Meyer<sup>ib</sup> <sup>b</sup> and Peter Faller<sup>ib</sup> <sup>\*a</sup>

Ru complexes are widely studied in photodynamic therapy. The type I mechanism of action is based on a photoinduced electron transfer from the complex to  $\text{O}_2$  and needs an electron donor to be catalytic. Little is known about electron donors among physiologically relevant compounds. Hence, we investigated the oxidation of ascorbate, NADH, cysteine, and glutathione with the canonical  $[\text{Ru}(\text{bpy})_3](\text{PF}_6)_2$  as well as a derivative with a peripheral disulphide unit,  $[\text{Ru}(\text{S}^{\text{S}}\text{bpy})(\text{bpy})_2](\text{PF}_6)_2$ . The established reactivity order is ascorbate > NADH ~ cysteine > glutathione.

Ruthenium–ligand complexes (Ru–L) have been a research subject for various applications, including medicinal for anticancer activity.<sup>1,2</sup> Different strategies are employed, and some of them include photoactivation.<sup>3–6</sup> Such an approach allows selectivity by choosing the location of illumination. Several different mechanisms were described, including photoactivation, such as photodynamic therapy (PDT) and photoactivated chemotherapy (PACT).<sup>7</sup> PACT is based on a photo-activated release of a ligand. The more classical PDT is divided into two types: type I includes an electron transfer to  $\text{O}_2$  forming superoxide  $\text{O}_2^{\bullet-}$  (Scheme 1) and type II, based on an energy transfer to  $\text{O}_2$  to form singlet  $^1\text{O}_2$ .<sup>8</sup> A crucial difference in type I is that the photoexcited  $\text{Ru}(\text{III})\text{--L}^+$  undergoes a single electron transfer to  $\text{O}_2$ , generating the  $\text{Ru}(\text{III})\text{--L}$ . This species can subsequently be reduced back to  $\text{Ru}(\text{II})$  with the aid of a sacrificial single electron donor, thereby completing the catalytic cycle (Scheme 1). In this context, the presence of such electron donors promotes type I over type II.<sup>9,10</sup> However, little consideration has been given to the choice of electron donor in a cellular context. Several compounds with

strong electron-donating properties are present in high concentrations in a cellular environment. Thiols, including glutathione (GSH) and cysteines (Cys), whether in free form or within proteins, serve as exemplary electron donors. Their concentrations typically range from 0.5–10 mM for GSH and 30–250  $\mu\text{M}$  for free Cys.<sup>11,12</sup> Other examples are ascorbate or vitamin C ( $\text{AscH}^-$ ) at 1–5 mM and Nicotinamide-adenine dinucleotide (phosphate) ( $\text{NAD(P)H}$ ) around 1–10  $\mu\text{M}$  in the cytosol and 60–75  $\mu\text{M}$  in mitochondria.<sup>13,14</sup> The type of electron donor (reducing agent) is relevant for anticancer strategies, as depletion of GSH and NADH, as well as the general redox imbalance, are considered as an anticancer strategy.<sup>15,16</sup>

Here, two Ru complexes,  $[\text{Ru}(\text{bpy})_3]^{2+}$  (**1**) and  $[\text{Ru}(\text{S}^{\text{S}}\text{bpy})(\text{bpy})_2]^{2+}$  (**2**) (Scheme 1), have been studied and compared. Complex **1** is the canonical Ru–L, hence, it was used in our study. Complex **2**, which contains a peripheral disulphide unit,<sup>17</sup> was chosen to test the hypothesis that a redox-active S–S bond could play a catalytic role in GSH oxidation.<sup>18</sup> However, **2** generally had a lower activity (see below). These two complexes have distinct photophysical and redox properties. They differ by their excited state lifetimes, 800 ns for **1** and 109 ns for **2**, both reported in



**Scheme 1** Hypothetical mechanism of the oxidation of the reducing agent ( $S_{\text{red}}$ ) catalyzed by  $[\text{Ru}(\text{bpy})_3]^{2+}$  upon irradiation (left) and structure of the  $[\text{Ru}(\text{bpy})_3]^{2+}$  and  $[\text{Ru}(\text{S}^{\text{S}}\text{bpy})(\text{bpy})_2]^{2+}$  complexes (right).

<sup>a</sup> Institut de Chimie (UMR 7177) University of Strasbourg – CNRS4 rue Blaise Pascal, 67000 Strasbourg, France. E-mail: pfaller@unistra.fr

<sup>b</sup> Institute of Inorganic Chemistry, University of Göttingen, Tammannstrasse 4, D-37077 Göttingen, Germany

<sup>c</sup> Department of Chemistry and Biochemistry, National Chung Cheng University, 168 University Rd., Min-Hsiung, Chiayi 62102, Taiwan

<sup>†</sup> Electronic supplementary information (ESI) available. See DOI: <https://doi.org/10.1039/d5cc01702e>

<sup>‡</sup> These authors contributed equally.



acetonitrile, and the luminescence quantum yield for **2** is lower by an order of magnitude.<sup>17,19</sup> And while the first reduction potential of **1** is  $-1.66$  V (vs.  $\text{Fc}^{+/0}$  in acetonitrile; reduction being bpy-centered), the reduction of **2** is significantly shifted anodically (to around  $-1.15$  V) and is a  $2e^-$  process centered at the disulphide unit.<sup>17</sup>

Our results suggest that under intracellular relevant concentrations of the electron donors  $\text{AscH}^-$ , NADH, Cys, and GSH,  $\text{AscH}^-$  is the preferred electron donor and GSH the least active. First, the stability in water at pH 7.4 under aerobic conditions of **1** and **2** was assessed by monitoring their absorption spectra over time. The spectra remained unchanged over 1 h, suggesting their stability under the present conditions (Fig. S1, ESI†). Next, the oxidizing ability of **1** and **2** was investigated with and without irradiation over time under aerobic conditions, expecting  $\text{O}_2$  as an electron acceptor. Cys and GSH oxidation was followed *via* the 5,5'-dithiobis(2-nitrobenzoic acid) (DTNB) assay monitoring reduced thiols at 412 nm, while the absorption bands of NADH and reduced  $\text{AscH}^-$  were followed at 340 nm and 265 nm, respectively. The oxidation of  $\text{AscH}^-$  (Fig. 1), Cys, GSH, and NADH (Fig. S2, ESI†) was observed only when the reaction medium was irradiated. This confirms that **1** and **2** require photoactivation for their catalytic oxidation of the reducing agents. Then, the initial turnover frequencies of light-induced oxidation of  $\text{AscH}^-$ , NADH, Cys, and GSH were determined, and the obtained values are reported in Table 1.

Comparing the two complexes, it is observed that **1** is more efficient than **2** for each reducing agent which could be explained by the longer lifetime and/or higher quantum yield

of **1** vs. **2**. The order for **1** was  $\text{AscH}^- > \text{NADH} > \text{Cys} > \text{GSH}$ , with  $\text{AscH}^-$  being the fastest oxidized. For complex **2**,  $\text{AscH}^-$  was again the fastest, but then Cys was faster than NADH. Also, GSH tended to be faster, but the error was larger. Hence, in relative terms, **2** did better than **1** for Cys and GSH.

This could indicate that the disulfide in **2** might play an accelerating role in the case of thiol reductants. Because the effect was small and **2** is overall less active than **1**, no studies on the mechanism in case of **2** were performed, and further work focused on **1**. But a complex with longer lifetime and a disulfide bond might be of interest for future developments.

Oxidation of the substrates can, in principle, occur *via* two mechanisms: (i)  $^1\text{O}_2$  oxidizes the substrates after energy transfer from **1**, (ii) by  $\text{Ru(III)}$  after electron transfer to  $\text{O}_2$  but also by the reduced  $\text{O}_2$  species. To see if the formation of  $^1\text{O}_2$  played a major role, the reaction with GSH was investigated in more detail, as this is the slowest reaction and, hence the most likely to produce  $^1\text{O}_2$ . To that end, the reaction products were analyzed. Different oxidation products have been reported for GSH: disulfides (RSSR), as well as thiosulfinate esters (RSOSR), sulfinic ( $\text{RSO}_2\text{H}$ ), and sulfonic ( $\text{RSO}_3\text{H}$ ). The formation of  $\text{RSO}_2\text{H}$ , RSOSR, and  $\text{RSO}_3\text{H}$  is often assigned to the oxidation of a thiol by  $^1\text{O}_2$ .<sup>25,26</sup> The reaction was followed by analysing the products *via* HPLC (Fig. S3, ESI†). Only GSSG could be detected as a product. This indicates that the ROS produced occurs mainly *via* an electron (type I) and not an energy transfer under the present conditions. To confirm the result, the oxidation of GSH was also followed in the presence of anthracene (Fig. S4, ESI†), which acts as a trap to  $^1\text{O}_2$ . The absorption spectra of anthracene showed no enhanced change over time upon irradiation of **1** compared to irradiation without **1**, indicating that irradiation of **1** did not produce a significant amount of  $^1\text{O}_2$ . These experiments show that GSSG is the main product of the reaction, which is in line with  $\text{O}_2$  serving as an electron acceptor.

As mentioned above, if  $\text{O}_2$  is the electron acceptor, the substrates can be oxidized in two ways, by  $\text{Ru(III)}\text{-L}$  or by the reduced oxygen species formed. Upon electron acceptance,  $\text{O}_2$  will form  $\text{O}_2^{\bullet-}$  that can rapidly disproportionate to  $\text{O}_2$  and  $\text{H}_2\text{O}_2$ .



$\text{H}_2\text{O}_2$  reacts relatively sluggishly with GSH or  $\text{AscH}^-$  in the absence of a catalyst, but irradiation at 450 nm, as conducted

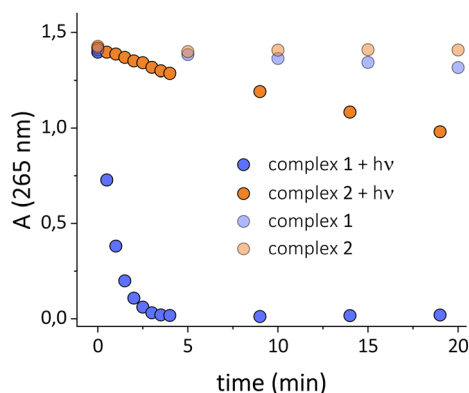


**Fig. 1**  $\text{AscH}^-$  oxidation followed by the decrease of its absorption peak at 265 nm with and without irradiation. Conditions: [**1**] and [**2**] 10  $\mu\text{M}$ ,  $[\text{AscH}^-]$  100  $\mu\text{M}$ , HEPES 100 mM, pH 7.4,  $\lambda_{\text{exc}}^{450\text{nm}}$ , 25  $^\circ\text{C}$ .

**Table 1** The initial turn-over frequency (TOF<sub>i</sub>) of complex **1** and **2** under radiation for different reducing agents, along with their  $\text{pK}_a$  values and redox potentials  $E^{\circ'}$  (vs. NHE). TOF<sub>i</sub> has been determined by dividing the initial rate by the concentration of the RuL complexes in the different experiments (10  $\mu\text{M}$  with  $\text{AscH}^-$  and NADH, and 30  $\mu\text{M}$  with Cys and GSH)

	TOF <sub>i</sub> $\pm$ SE (min <sup>-1</sup> )		$\text{pK}_a^{20,21}$	$E^{\circ'}$ 2e <sup>-</sup> (mV)			
	<b>1</b>	<b>2</b>		$E^{\circ'}$ 1st (mV) <sup>22,23</sup>	$E^{\circ'}$ 2nd (mV) <sup>22,23</sup>	Calculated	Literature <sup>11,24</sup>
AscH	16.20 $\pm$ 0.24	0.86 $\pm$ 0.04	4.2	+282	-174	+54	+66
NADH	6.8 $\pm$ 0.24	0.22 $\pm$ 0.02	—	+282	-922	-320	-315
Cys	3.08 $\pm$ 0.06	0.41 $\pm$ 0.01	8.3	+920	-1500	-290	-240
GSH	0.99 $\pm$ 0.20	0.35 $\pm$ 0.16	8.9	+920	-1500	-290	-220



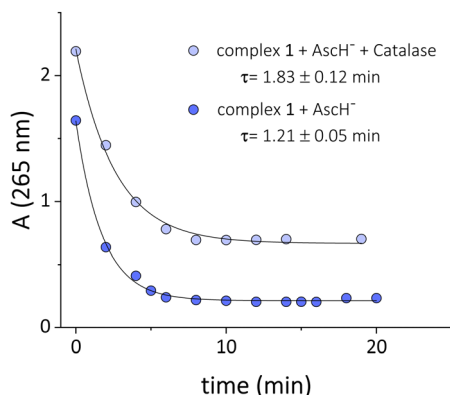


Fig. 2 AsCH<sup>−</sup> oxidation catalyzed by complex **1** followed at 265 nm w/w/o catalase. Conditions: [**1**] 10 μM, [AsCH<sup>−</sup>] 100 μM, [Catalase] 2 μM, HEPES 100 mM, pH 7.4, λ<sub>exc</sub><sup>450nm</sup>, 25 °C.

here, might accelerate the reaction. Hence, reaction with H<sub>2</sub>O<sub>2</sub> could contribute to the substrate oxidation in the presence of Ru-L. To isolate this effect, AsCH<sup>−</sup> oxidation by **1** was monitored with catalase (Fig. 2), which breaks down H<sub>2</sub>O<sub>2</sub>. The results show that AsCH<sup>−</sup> oxidation is slowed by a factor of about 1.5. This suggests that indeed, reaction (2) contributes to the oxidation.

After investigating the activity of different substrates individually, it was interesting to investigate the selectivity of the complex toward different substrates present simultaneously, as expected in a cell. First, the fastest AsCH<sup>−</sup> was investigated. The rate of AsCH<sup>−</sup> oxidation was little affected by the addition of equivalent concentrations of NADH or a tenfold excess of GSH (Fig. 3). The plateau of the AsCH<sup>−</sup> peak is reached at the same time as that in the case of AsCH<sup>−</sup> alone. Here, it is important to note that NAD<sup>+</sup> absorbs around the same spectral region as AsCH<sup>−</sup> (265 nm). As AsCH<sup>−</sup> is consumed, NAD<sup>+</sup> is produced. Hence, the plateau of the absorption at 265 nm is reached at a higher absorption value.

In contrast, when monitoring NADH oxidation under the same conditions, the absorptions of AsCH<sup>−</sup> and its product do not interfere. Adding AsCH<sup>−</sup> slowed down NADH oxidation (Fig. 3), hence corroborating the predominant oxidation of AsCH<sup>−</sup> over NADH in a direct competition. A similar result is observed in the case of GSH, even at concentrations of 0.1 mM

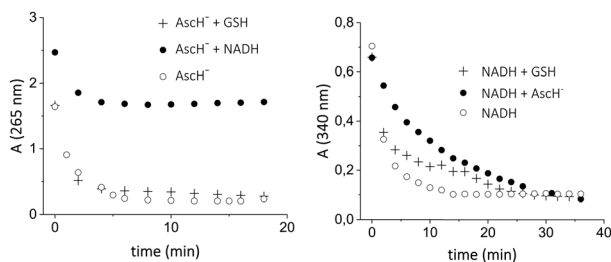


Fig. 3 Kinetic of AsCH<sup>−</sup> (left) and NADH (right) oxidation catalyzed by **1** under irradiation in the presence of GSH and each other followed by the absorbance at 265 nm and 340 nm, respectively. Conditions: [**1**] 10 μM, [AsCH<sup>−</sup>] 100 μM, [NADH] 100 μM, [GSH] 1 mM, HEPES 100 mM, pH 7.4, λ<sub>exc</sub><sup>450nm</sup>, 25 °C.

AsCH<sup>−</sup> and 1 mM GSH. This supports that the order of oxidation rate is also maintained in a mixture, and AsCH<sup>−</sup> is preferred.

Another aspect is the role of Cys. It has been shown that Cys can accelerate GSH oxidation *via* a disulfide exchange in the case of oxidation by CuCl<sub>2</sub>.<sup>27</sup> Hence, the oxidation of Cys and GSH in two different molar proportions was followed (Fig. 4). In the case where the two thiols are equimolar (0.5 mM each), the oxidation of thiols is fast, leaning toward Cys kinetics. This is in line with the idea that the presence of Cys accelerates the overall oxidation of free thiols. This can be explained by the fact that Cys is oxidized faster and in turn, can further oxidize GSH *via* disulfide exchange and *via* the produced ROS. However, it was observed that the kinetics of the mixture of the two thiols resemble that of GSH oxidation alone when the ratio of GSH to Cys is 10 : 1, with concentrations of 1 mM and 0.1 mM, which are typical values in the cytosol of a cell. When the oxidation of GSH was followed in the presence of AsCH<sup>−</sup> with a concentration of 1 mM and 100 μM, respectively (10 : 1), it was observed that the kinetics of GSH oxidation was left unaffected relative to the case where only GSH was present.

Overall, the data are in line with the order AsCH<sup>−</sup> > NADH > Cys > GSH for oxidation by the light-induced reaction of **1** aerobically. This order is maintained when two substrates are present simultaneously. This can be explained by an outer sphere electron transfer from the substrate to the Ru(III). Otherwise, the coordination strength to Ru(II) would be expected to play a role, and thiolates are expected to bind stronger than NADH or AsCH<sup>−</sup> (and GSH stronger than Cys). Moreover, no spectral change in absorption (Fig. S1, ESI<sup>†</sup>) upon the addition of the substrates to **1** or **2** was observed, suggesting no coordination to **1** or **2**, which is expected from the saturated coordination sphere of Ru(II). To explain the order, an obvious parameter is the redox potential (Table 1). As the mechanism involves a single electron transfer, the relevant redox potential is the single electron oxidation of the substrates. This is much lower for NADH and AsCH<sup>−</sup> compared to the thiols.<sup>22,23</sup> Concerning the differences in reaction rate between GSH and Cys (Fig. 4), they are often explained *via* the fraction of thiolates available at a

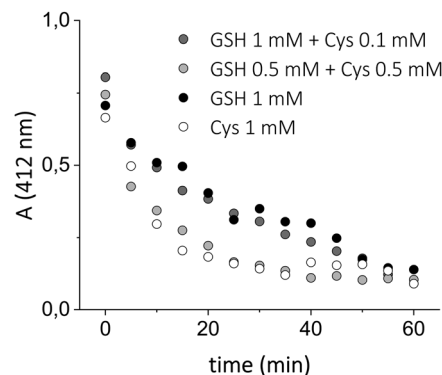


Fig. 4 Kinetic of GSH oxidation catalyzed by **1** under irradiation in the presence of Cys monitored by DTNB assay (absorption peak at 412 nm). Conditions: [**1**] 30 μM, [GSH] and [Cys] 0.1–1 mM, HEPES 100 mM, pH 7.4, λ<sub>exc</sub><sup>450nm</sup>, 25 °C.



given pH, based on the idea that the thiolates are the active form. The  $pK_a$  of GSH and Cys is 8.9 and 8.3, respectively, and therefore at pH 7.4, the fraction of thiolate ( $f_{RS^-}$ ) is 0.028 and 0.112 ( $f_{RS^-}$  is defined as  $f_{RS^-} = (10^{(pK_a - pH)} + 1)^{-1}$ ).<sup>21</sup> If this is the only relevant factor, Cys should be about 4 times faster, but in fact, Cys oxidation is much faster, indicating that other factors also play a role. Hence, the oxidation order can't be explained straightforwardly. Other parameters might be involved, such as steric hindrance or electrostatic interactions. The latter could explain the difference between AsCH<sup>−</sup> and NADH.

A key area of research involving  $[Ru(bpy)_3]^{2+}$  focuses on synthesizing potential photoactivable anticancer agents by producing ROS. It is broadly accepted that the depletion of intracellular reducing agents, such as GSH, is an anticancer strategy, but the basic mechanism has not been really addressed, and the electron donors are not known. Here, two  $[Ru(bpy)_3]^{2+}$  type complexes were studied, and their oxidative properties toward four biologically relevant substrates, isolated and in combination, were investigated. Considering the average concentration in a human cytosol, AsCH<sup>−</sup> would be the most plausible electron source for **1** among the substrates studied. Hence, depletion of AsCH<sup>−</sup> would occur fastest, which in turn could then lead to depletion of GSH/NAD(P)H as these are the substrates for the enzymatic re-reduction of oxidized ascorbate. The present data indicate that not only the depletion is the fastest with AsCH<sup>−</sup>, but it is also associated with the formation of superoxide, which in turn leads to more oxidation. Hence, the presence of AsCH<sup>−</sup> would also lead to faster ROS production. This is of importance as the AsCH<sup>−</sup> concentrations vary between different types of cells in an organism and can depend on the state of a cell, or for instance, AsCH<sup>−</sup> is absent in bacteria. This could lead to different susceptibility to photocatalytic oxidation with **1**. Such consideration might also be extended to other photocatalytic complexes of Ru or other metal ions.

Methodology – I. D., D. O., S.-A. H., V. L., F. M., P. F.; formal analysis – I. D., D. O., P. F.; investigation physicochemistry – I. D., D. O.; investigation synthesis – S.-A. H.; writing original draft – I. D., D. O., review & editing – I. D., S.-A. H., F. M., P. F.; supervision – F. M., V. L., P. F.; conceptualization – P. F.

Dr M. Desage-El Murr (Strasbourg) is acknowledged for helpful discussions and drawing our attention to the existence of **2**. We thank Dr M. Seemann (Strasbourg) for providing NADH and M. Oelschlegel (Göttingen) for sending the compounds. This work was supported by the Interdisciplinary Thematic Institute SysChem, *via* the IdEx Unistra (ANR-10-IDEX-0002) (to P. F.), by the CSC Graduate School (CSC-IGS ANR-17-EURE-0016) (to D. O.) within the French Investments for the Future Program, by the German Research Foundation (DFG) *via* project ME 1313/15-2 (404391096) within the SPP 2102 and by the Institut Universitaire de France (to P. F.).

## Data availability

The data supporting this article have been included as part of the ESI.† Absorbance data can be available upon request.

## Conflicts of interest

There are no conflicts to declare.

## Notes and references

- G. Gasser and N. Metzler-Nolte, *Curr. Opin. Chem. Biol.*, 2012, **16**, 84–91.
- B. Perillo, M. Di Donato, A. Pezone, E. Di Zazzo, P. Giovannelli, G. Galasso, G. Castoria and A. Migliaccio, *Exp. Mol. Med.*, 2020, **52**, 192–203.
- K. M. Kuznetsov, K. Cariou and G. Gasser, *Chem. Sci.*, 2024, **15**, 17760–17780.
- L. Conti, E. Macedi, C. Giorgi, B. Valtancoli and V. Fusi, *Coord. Chem. Rev.*, 2022, **469**, 214656.
- S. Monro, K. L. Colón, H. Yin, J. Roque, P. Konda, S. Gujar, R. P. Thummel, L. Lilge, C. G. Cameron and S. A. McFarland, *Chem. Rev.*, 2019, **119**, 797–828.
- C. Mari, V. Pierroz, S. Ferrari and G. Gasser, *Chem. Sci.*, 2015, **6**, 2660–2686.
- D. M. Arias-Rotondo and J. K. McCusker, in *Visible Light Photocatalysis in Organic Chemistry*, Wiley, 2018, 1–24.
- D. E. J. G. J. Dolmans, D. Fukumura and R. K. Jain, *Nat. Rev. Cancer*, 2003, **3**, 380–387.
- M. S. Baptista, J. Cadet, P. Di Mascio, A. A. Ghogare, A. Greer, M. R. Hamblin, C. Lorente, S. C. Nunez, M. S. Ribeiro, A. H. Thomas, M. Vignoni and T. M. Yoshimura, *Photochem. Photobiol.*, 2017, **93**, 912–919.
- M. S. Baptista, J. Cadet, A. Greer and A. H. Thomas, *Photochem. Photobiol.*, 2021, **97**, 1456–1483.
- F. Q. Schafer and G. R. Buettner, *Free Rad. Biol. Med.*, 2001, **30**, 1191–1212.
- L. P. Osman, S. C. Mitchell and R. H. Waring, *Sulfur Rep.*, 1997, **20**, 155–172.
- E. Falcone, F. Stellato, B. Vilen, M. Bouraguba, V. Lebrun, M. Ilbert, S. Morante and P. Faller, *Metallomics*, 2023, **15**, mfad040.
- G. H. Patterson, S. M. Knobel, P. Arkhammar, O. Thastrup and D. W. Piston, *Proc. Natl. Acad. Sci. U. S. A.*, 2000, **97**, 5203–5207.
- B. Niu, K. Liao, Y. Zhou, T. Wen, G. Quan, X. Pan and C. Wu, *Biomaterials*, 2021, **277**, 121110.
- H.-Q. Ju, J.-F. Lin, T. Tian, D. Xie and R.-H. Xu, *Sig. Trans. Target Ther.*, 2020, **5**, 231.
- S.-A. Hua, M. Cattaneo, M. Oelschlegel, M. Heindl, L. Schmid, S. Dechert, O. S. Wenger, I. Siewert, L. González and F. Meyer, *Inorg. Chem.*, 2020, **59**, 4972–4984.
- M. Huang, J. Cui, Q. Wu, S. Liu, D. Zhu, G. Li, M. R. Bryce, D. Wang and B. Z. Tang, *Inorg. Chem.*, 2024, **63**, 24030–24040.
- M. Heindl, J. Hongyan, S.-A. Hua, M. Oelschlegel, F. Meyer, D. Schwarzer and L. González, *Inorg. Chem.*, 2021, **60**, 1672–1682.
- C. L. Linster and E. Van Schaftingen, *FEBS J.*, 2007, **274**, 1–22.
- C. C. Winterbourn and D. Metodiewa, *Free Rad. Biol. Med.*, 1999, **27**, 322–328.
- R. F. Anderson, *Biochim. Biophys. Acta*, 1980, **590**, 277–281.
- G. R. Buettner, *Arch. Biochem. Biophys.*, 1993, **300**, 535–543.
- H. Borsook and G. Keighley, *Proc. Natl. Acad. Sci. U. S. A.*, 1933, **19**, 875–878.
- G. Frison and G. Ohanessian, *J. Comput. Chem.*, 2008, **29**, 416–433.
- T. P. A. Devasagayam, A. R. Sundquist, P. Di Mascio, S. Kaiser and H. Sies, *J. Photochem. Photobiol. B*, 1991, **9**, 105–116.
- I. Doumi, L. Lang, B. Vilen, M. Deponte and P. Faller, *Chem. Eur. J.*, 2024, **30**, e202304212.

